Roughening during XeF2 etching of Si(100) through interface layers : H:Si(100) and a-Si/Si(100)

Roughening during XeF_2 etching of Si(100) through interface layers: H:Si(100) and *a*-Si/Si(100)

A. A. E. Stevens, M. C. M. van de Sanden, H. C. W. Beijerinck, and W. M. M. Kessels[a)]
Department of Applied Physics, Eindhoven University of Technology, P.O. Box 513, 5600 MB Eindhoven, The Netherlands

(Received 5 May 2008; accepted 26 January 2009; published 27 February 2009)

Real-time spectroscopic ellipsometry has been applied *in situ* in an Ar^+/XeF_2 beam-etching experiment to study the roughening of Si(100) etched by XeF_2 at room temperature. The role of initial surface conditions has been examined. For the etching of hydrogen-terminated (H:)Si(100), the roughness evolution as a function of XeF_2 dose can be characterized by an initially fast roughening phase followed by a slower, final roughening phase. Similar behavior is observed when etching through an amorphous silicon (*a*-Si) layer on top of crystalline Si(100) bulk as obtained by sputter cleaning of Si(100) substrates. These observations can be explained as follows. Both H termination and *a*-Si lead to patch formation on the surface where etching is impeded and hence, high aspect-ratio etch pits develop. The quantitative differences in roughening can then be attributed to the duration and timing of the influence of the H-terminated and *a*-Si patches on the etch process until H-bonded Si surface atoms or *a*-Si are totally removed from the surface. Surface area increase due to the roughening can therefore be held responsible for observed trends and differences in etch rates, reaction layer thickness, and composition as a function of etch time. © *2009 American Vacuum Society.* [DOI: 10.1116/1.3085718]

I. INTRODUCTION

Fundamental studies of dry etching of silicon are of great interest considering its role in semiconductor fabrication. Key issue in the chemical processing of silicon surfaces is to produce well-defined, low-damage surfaces. Better understanding of the atomic-scale reaction dynamics between halogens and Si(100) surfaces can aid in meeting these technological demands for next generation semiconductor devices.

Initial surface conditions prior to processing can be of significant importance for the etch process, whether the surface is clean and reconstructed, hydrogen-terminated, sputter cleaned by ion bombardment or contaminated.[1–4] Furthermore, spontaneous chemical etching is an isotropic etch process in which roughening of the surface is a major concern. Often, roughness has been used as an argument in literature to explain some not well understood experimental observations.[2,5–7] Insight into the fundamentals of roughening of surfaces and the influence of initial surface conditions in etch processing is required to increase the understanding of the microscopic etch mechanisms.

In a first study we have already shown that surface roughening is severe when etching sputter-cleaned Si(100) with XeF_2 using single-wavelength ellipsometry.[3] Here, the roughening mechanism of silicon etched by XeF_2 has been studied by applying *in situ*, real-time spectroscopic ellipsometry (SE) in a Ar^+/XeF_2 beam-etching apparatus for various initial surface conditions: XeF_2 etching of (a) hydrogen-terminated Si(100) [H:Si(100)] and (b) Ar^+ sputter-cleaned, amorphous silicon (*a*-Si) on top of a *c*-Si(100) bulk [*a*-Si/Si(100)]. In this way we can study how initial surface conditions may have an impact on the roughening mechanism and, additionally, by using spectroscopic ellipsometry instead of single-wavelength ellipsometry we may obtain more detailed information on the roughness characteristics.

First, some aspects of the XeF_2 etch mechanism of silicon will be addressed (Sec. II) Next, the experimental details are discussed (Sec. III), followed by a description of the multilayer dielectric models that have been used to analyze the SE measurements (Sec. IV). Then, two case studies will be described: (a) the etching of H:Si(100) in Sec. V, including a comparison with atomic-force-microscopy measurements, and (b) the etching of *a*-Si/Si(100) in Sec. VI. Differences and similarities between the two cases as well as implications for the XeF_2/Si etch mechanism will be discussed in Sec. VII.

II. XeF_2/Si ETCH MECHANISM

Surface roughness and initial surface conditions might be responsible for some of the conflicting experimental observations within the framework of the XeF_2/Si etch mechanism. A brief overview of key elements of the reaction mechanism at room temperature will be presented here, including the issues of initial surface conditions and the potential influence of surface roughness.

A. Initial reaction steps

In the case of a clean Si surface, a F atom is abstracted from the XeF_2 molecule by a reactive site, i.e., dangling bond, without energy barrier, whereby the complementary XeF scatters off the surface.[8] As a result, the surface layer consists initially primarily of SiF for most reconstructed

a)Electronic mail: w.m.m.kessels@tue.nl

TABLE I. Reaction layer thicknesses and SiF_x-species distributions as reported in literature. The silicon surfaces were all (2×1) reconstructed prior to processing unless mentioned otherwise. The total coverages marked with an asterisk (*) are estimates by the authors from species coverage ratios as the references do not give quantitative measure for the total coverage.

Initial surface	Ref.	Species coverage ratios $SiF:SiF_2:SiF_3$	Total coverage (ML)	XeF_2 dose (ML)
Si(100), 10 Ω cm	21	3.00:1:0.28	1.13	50
Si(100)	12	2.00:1:0.25	1.40	50
sputtered Si(100), 10 Ω cm	21	1.25:1:0.25	1.13	50
Si(111)-(7×7) 1 Ω cm	7	2.78:1:1.56	0.95	10^3
Si(111)-(7×7) 1 Ω cm	7	1.78:1:1.95	1.75	$>10^4$
H-terminated So(111), 10 Ω cm	2	3.25:1:5.50	3.6 *	$>10^4$
n- and *p*-doped Si(111), 0.1 Ω cm	22	1.58:1:3.71	2.5 *	$>10^4$
n-doped Si(111), 0.001 Ω cm	22	1.74:1:4.07	2.7 *	$>10^4$
p-doped Si(111), 0.001 Ω cm	22	1.67:1:4.37	2.8 *	$>10^4$

Si(100) and Si(111) surfaces with possibly some SiF_2 at step edges. Once dangling bonds are passivated, the next reaction step requires breaking of Si–Si backbonds which is an activated process with a much smaller reaction probability. Since F is known to be very electronegative, bond charges will reside preferentially close to the F atom, leading to an effective charge separation between the Si (δ^+) and F (δ^-).[9] The backbonds are weakened by this phenomenon and, hence, backbonds are susceptible to subsequent F-atom insertion, which is supplied by physisorbed XeF_2 molecules, or as proposed by Morikawa *et al.*[2] and Winters *et al.*,[10] by F^- atoms already interstitially present in between the Si lattice atoms. Subsequent steps of F-atom attachment to SiF_x surface species leads eventually to the formation of SiF_4 molecules, which are volatile and can desorb from the surface as the main etch product at room temperature,

$$\mathrm{Si} \xrightarrow{+F} \mathrm{SiF} \xrightarrow{+F} \mathrm{SiF_2} \xrightarrow{+F} \mathrm{SiF_3} \xrightarrow{+F} \mathrm{SiF_4}(g). \quad (1)$$

The silicon fluoride reaction layer thickness remains this way typically 1.5 ML (monolayer),[11] composed of a surface layer of SiF and SiF_2 species (partially) covered by a layer of SiF_2/SiF_3 species.

Table I lists a selection of literature reports on species coverages and reaction layer thicknesses. Clearly, some variations in observations are visible, possibly because of different XeF_2 exposure times, preparation method, and doping level of the Si substrates. After a low (50 ML) XeF_2 dose, surfaces are primarily SiF, whereas SiF_3 is a minority species. Hence, SiF_4 products are not easily produced and the etch rate/reaction probability is very low.[12] After 50 ML of dose the surface is still flat since relatively little etching has occurred. Lo *et al.* showed that it takes about 10^3 ML of XeF_2 dose to reach an intermediate, steady-state reaction layer consisting of primarily SiF followed by SiF_3 and a minor amount of SiF_2.[7] Hence, the experiments and simulations remaining far below 10^3 ML of XeF_2 exposure may still be categorized as being in the process of reaction layer build-up despite the fact that during this process etching may already have occurred. Continued exposure to XeF_2, beyond a 10^3 ML dose, shows an increase in all species and the increase is most pronounced in the SiF_3 species coverage, which becomes by far the most abundant species.[7] Due to the removal of Si in the etch process, the surface is believed to roughen and hence, the total amount of SiF_x species increases. One can argue that surface area increase due to roughening allows more SiF_3 to be present on the surface, whereas on flat surfaces only a small amount is allowed due to steric hinderance. Thus, defining a reaction layer composition seems to be arbitrary if the total XeF_2 dose and/or the surface morphology are not known.

B. Influence of initial surface

Initial surface conditions have also a significant effect on both the initial reaction of F with Si and on the etch process on longer times scales. Morikawa *et al.* observed similar trends and ratios in species coverage as a function of XeF_2 dose as reported by Lo *et al.*, although in this case the initial surface is H terminated.[2] The SiF_x growth occurrence on H-terminated Si(100) shows, however, a delay for about 0.5×10^3 ML. The H-terminated surface is apparently stable for a prolonged period of time. The fact that Si(100) is not etched in hydrofluoric acid (HF) treatment and leads to H-terminated Si(100) is already an indicator for the fact that H-terminated Si(100) is an energetically favorable and more stable surface state than F-terminated Si(100).[13] The hydrogen is not replaced by F, but needs to be removed by SiH_xF_y product formation. The F atoms need to be inserted into the subsurface back-bonds of the first Si layer to achieve this. Now, once a SiH_xF_y is released at a certain position on the surface, SiF species in the next layer can be exposed to incoming XeF_2 molecules, and the regular etching can start. The observed presence of H–Si bonds even after exposure to XeF_2 above $\sim10^4$ ML substantiates the fact that H is not easily removed from the Si surface.[2]

A different initial surface condition can be obtained by sputter cleaning. A sputter-cleaned Si(111) shows already a totally different reaction layer after 50 ML of XeF_2 dose as compared to a (2×1)-reconstructed Si(100) surface (Table I), possibly because of the amorphous surface structure. Initial reaction of F with surface atoms is not hampered, a reaction layer is formed and the etching can start immediately. Next, the *a*-Si is being removed, resulting in a gradually increasing roughness.[3] Once the etching arrives at the *a*-Si/*c*-Si interface, at some positions on the surface the *c*-Si is going to be etched while at other positions *a*-Si remains as patches on the surface. For this case, we showed that roughening of the surface is in fact an important aspect of the etch process and also, that the etch rate is enhanced as a result of surface morphology changes.[3] Furthermore, it was shown that the buried amorphous-crystalline interface plays a major role in the roughening dynamics. The real-time SE experiments presented in this article should be able to show the

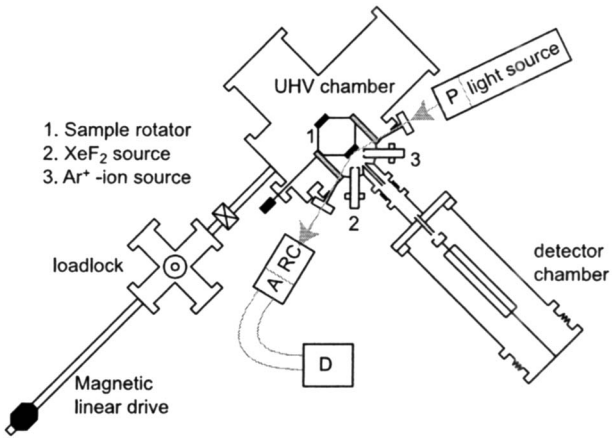

FIG. 1. Experimental setup in horizontal cross section. Samples can be exchanged between a rotatable sample holder and the sample storage in the load lock with a linear magnetic drive. The sample is mounted in a rotatable sample holder (1) that can be operated manually via an external drive. The XeF_2 source (2) and Ar^+-ion source (3) are at 52° and 45° from surface normal, respectively. Etch products are detected in a separate detector chamber perpendicular to the sample surface. The spectroscopic ellipsometer is incident at 74.3° from the surface normal. The SE consists of a broadband light source, polarizer (P), rotating compensator (RC), analyzer (A); and a fiber-coupled charge coupled device-array detector (D).

implications of roughening and initial surface conditions on some of the experimental observations for the etching of silicon with XeF_2.

III. EXPERIMENTAL DETAILS

The experimental setup used in this study has been described extensively in previous publications. Figure 1 shows a cross section of the setup. The new feature is the addition of a spectroscopic ellipsometer (Woollam M-2000U with an infrared extension) covering the photon energy range of 0.75–5 eV (250–1700 nm). The angle of incidence is typically 74.3° with respect to the surface normal and the light is focused onto a 1 mm^2 area of the sample. Each measured spectrum is an average over typically 200 spectra recorded by the ellipsometer resulting in a time resolution of typically 10 s, which is more than sufficient for the experiments described in this article. The spectroscopic ellipsometry data are analyzed with WVASE32® software. All measurements have been performed at room temperature.

Simultaneously with the ellipsometry measurements, etch products are monitored with the mass spectrometer. At room temperature the only etch product for the etching of Si(100) with XeF_2 is SiF_4.[6,14] The SiF_3^+ signal is a measure for the SiF_4 etch product flux and is converted in the production coefficient δ,[3] which is defined as

$$\delta = \frac{2\Phi(SiF_4)}{\Phi_s(XeF_2)}, \tag{2}$$

with $\Phi_s(XeF_2)$ the impinging flux on the sample and $\Phi(SiF_4)$ the product flux leaving the sample. The production coefficient or etching efficiency is defined such that $\delta=1$ corresponds to the full conversion of reactant into products. It should be noted that differences in absolute value of δ between various literature reports can be observed due to calibration differences over the course of years, however, the experiments presented in this report can be compared in absolute sense.

For the H-terminated *c*-Si etching experiments the native oxide is removed by dipping 10×10 mm^2 Si(100) substrates in a 2% hydrofluoric acid (HF) solution for 2 min after ultrasonic cleaning with ethanol at 40 °C and rinsing in purified water. This leads to a mono-, di-, and trihydride-terminated Si substrates with mostly dihydrides.[13] Furthermore, SE shows an initial roughness/steps of typically 6 ML and ~0.15 nm root-mean-square roughness measured with atomic force microscopy (NT-MDT Solver P47) in noncontact mode (scan size: 1.5×1.5 μm).

For the *a*-Si/*c*-Si transition etch experiment, the samples are ultrasonically cleaned with ethanol at 40 °C, rinsed with purified water and *in situ* bombarded with 1 keV Ar^+ ions to remove the native oxide and create a 6.4 nm *a*-Si top layer. The Si(100) used in this study is phosphorus-doped *n*-type Si with a resistivity of 10–30 Ω cm.

IV. MULTILAYER DIELECTRIC MODEL

Two differently prepared Si(100) samples have been etched with XeF_2: a H-terminated Si(100) sample and a sputter-cleaned Si(100) sample. To obtain information from SE measurements, different multilayer dielectric models for the substrates have to be used, as described next.

A. H-terminated Si(100)

The multilayer dielectric model for the substrate consists of a stack of layers on top of the *c*-Si-bulk substrate, with different dielectric functions for the materials in the various layers. For *c*-Si the dielectric functions described by Jellison and Modine[15] are used. Often, a single roughness layer is included in multilayer models with 0.5 void fraction and 0.5 material fraction. The Bruggemann effective medium approximation is then used to calculate the effective dielectric functions for the roughness layer.[16] As will be discussed below, we have chosen to model the roughness using a two-layer roughness model to fit the ellipsometry measurements, with 0.75 void/0.25 *c*-Si fractions in the top layer and 0.25 void/0.75 *c*-Si fractions in the bottom layer, as shown in Fig. 2.

Measured pseudodielectric functions $\langle\epsilon_1(\omega)\rangle$ and $\langle\epsilon_2(\omega)\rangle$, as derived from the measured ellipsometric angles $\Psi(E)$ and $\Delta(E)$ (Ref. 17) assuming a two-phase (ambient/substrate) layer model, have been plotted in Fig. 3.

Typical root-mean-square experimental errors are $\sigma_{\epsilon_1}=\sigma_{\epsilon_2}=0.05$. For reference, the dielectric function of silicon is shown. The absolute $\langle\epsilon_1(\omega)\rangle$ shows a gradual decrease over the full spectra range. Below $E(\omega)=2.5$ eV, the function $\langle\epsilon_2(\omega)\rangle$ shows an increase with increasing XeF_2 dose; above $E(\omega)=2.5$ eV, the function $\langle\epsilon_2(\omega)\rangle$ shows a decrease with increasing XeF_2 dose. Fit optimization with the two-layer roughness model is done by minimizing the χ^2 between experimental and calculated pseudodielectric functions. The

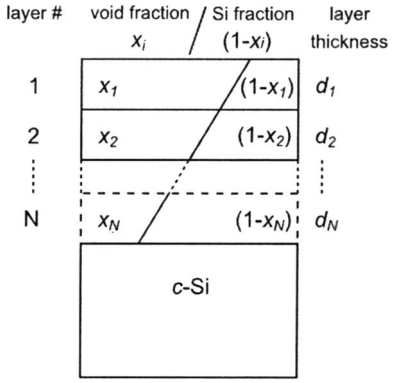

FIG. 2. Multilayer roughness modeling. Layer i with thickness d_i has a void percentage x_i, which is always larger than the void percentage x_{i+1} of the lower lying layer $i+1$. Using this model, the morphology details of the roughness layer can be included in the analysis of the experimental results.

value of χ^2 for the fits gradually increases from $\chi^2=4$ for the initial H-terminated Si substrate up to $\chi^2=12$ for long XeF_2-exposure times.

Including multiple layers for the roughness is necessary because of the structure dependence of the rough layer during etching. This was already observed in an earlier study using single-wavelength ellipsometry,[3] where the void fraction in a single roughness layer modeling was used to properly model the ellipsometry measurement. To further support the multilayer roughness modeling approach, a fit analysis for a set of multilayer models of a H:Si(100) sample after exposure to 1.2×10^4 ML XeF_2 has been performed and is summarized in Table II.

Large disagreement between measured and simulated SE spectra was observed when using a single roughness layer, with either a fixed or a fitted void fraction in the top layer, as can be concluded from the large $\chi^2>60$. Hence, including the void fraction in the fits is not sufficient in the SE measurements. A dramatic decrease in χ^2 can be observed when choosing two roughness layers. The χ^2 value is further reduced when choosing more layers and fitting the void fraction simultaneously. Choosing more layers and including void percentage fitting also implies having more fit parameters available. A larger number of fit parameters can result in better fits in terms of χ^2, but may not be reliable due to correlations between fit parameters, which is reflected in an increase in the 90% confidence interval value. Furthermore, the sum of the separate roughness layer thicknesses $\Sigma_i d_i$ increases with increasing number of layers.

Increasing the number of roughness layers included in the modeling results in capturing finer details of the roughness layer, i.e., higher peaks and deeper valleys. Due to this effect, a weighting method of the separate layers is introduced to be able to make a comparison between fit results with multiple layers. The weighting method translates the multilayer thicknesses into a single-layer thickness, as follows:

$$d_r = \sum_{i=1}^{N} g_i d_i, \tag{3}$$

where the weighting factor g_i is related to the void fraction x_i

$$g_i = 1 - |1 - 2x_i|, \tag{4}$$

such that the contribution of layers situated far from the mean heights, i.e., tails of the total height distribution, is reduced. This weighting method results in a weighted layer thickness d_r approximately equal and independent of the number of layers for all multilayer fits, as is shown in Table II.

In conclusion, the use of the multilayer roughness model is validated, where the weighted roughness layer thickness is comparable to the thickness of the roughness layer obtained assuming a single roughness layer model. The difference however is that specific morphology changes are accounted for as is necessary in this particular study. As the optimum choice for minimizing both the value of χ^2 and the number of parameters in the curve fit, we have chosen the two-layer model with fixed void fractions, 0.75 for the top layer, and 0.25 for the bottom layer. It should also be noted that the observed time dependence of the roughening as presented below was found to be independent of the number of layers included in the modeling. The weighted roughness layer thickness is used in the presentation and discussion of the results.

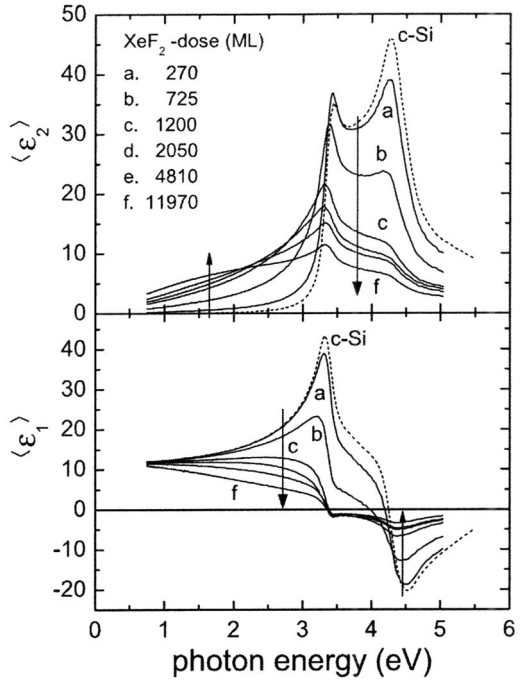

FIG. 3. Measured pseudodielectric functions (solid lines) after increasing exposure of H:Si(100) to XeF_2 using the two-layer roughness model. The arrows indicate the change in the various parts of the spectra as a function of XeF_2-exposure time. For reference the dielectric functions of c-Si are also shown (dashed lines).

TABLE II. Multilayer roughness modeling results (shown in Fig. 2) for the pseudodielectric functions measured after 1.2×10^4 ML XeF_2 dose on H:Si(100). The void fractions shown are the x_i from top layer to bottom layer and d_r is the weighted roughness layer thickness. If the void fractions are included as fit variable in the SE analysis it is mentioned in the void fraction column. Corresponding χ^2 values and the 90% confidence interval for d_r are a measure for the quality of the least squares curve fit. The simulation labeled (c) corresponds to the model chosen for the analysis of the real-time SE measurements as presented in the remainder of this article.

Simulation No.	No. of layer N	Void fraction x_i (top/…/bottom)	$\Sigma_i d_i$ (nm)	d_r (nm)	χ^2	90% confidence interval (nm)
(a)	1	0.50	17.8	17.8	83	0.2
(b)	1	0.57 (fit)	17.4	15.0	64	0.1
(c)	2	0.75/0.25	29.4	14.7	12	0.1
(d)	2	0.75/0.22 (fit)	31.0	14.5	11	0.2
(e)	3	0.90/0.50/0.10	44.2	18.3	8	0.3
(f)	3	0.93/0.57/0.13 (fit)	43.5	17.0	5	0.8
(g)	4	0.90/0.60/0.40/0.10	41.6	17.1	5	0.3
(h)	4	0.93/0.66/0.25/0.4 (fit)	52.7	16.1	4	1.4
(i)	5	0.90/0.70/0.50/0.30/0.10	40.6	17.8	5	1.0
(j)	5	0.96/0.68/0.48/0.22/0.03 (fit)	58.4	16.4	3	10

B. *a*-Si/Si(100)

For the analysis of the *a*-Si/Si(100) etch experiments two separate multi-layer models are used. The layer model used to fit the SE data is initially a single roughness layer of 0.5 void/0.5 *a*-Si on top of a *a*-Si layer with a *c*-Si substrate underneath. This model fails to fit the data properly once most of the *a*-Si is removed from the surface and predominately the underlying *c*-Si bulk is being etched. This is the point where the two-layer roughness model described above is used to fit the long term etching. To be able to quantitatively compare the roughness layer thickness for the two models, the weighted roughness layer thickness is again used. For *a*-Si the dielectric model is a Tauc-Lorentz model, which is commonly used for modeling amorphous materials.[18] This layer modeling approach is similar to the modeling approach of the single-wavelength ellipsometry experiments.[3]

V. H:SI(100) ETCHING

The real-time SE data fitted with the two-layer model and for fixed void percentages lead to the (weighted) roughness layer thickness d_r of the XeF_2 etched H:Si(100) as a function of XeF_2 dose, as shown in Fig. 4(a). The thickness of the separate layers d_{top} and d_{bottom} is shown as well. Figure 4(b)shows the production coefficient δ, which is proportional to the SiF_4-product flux. An impinging XeF_2 flux of 0.8 ML s^{-1} has been used. For about 500 ML of XeF_2-dose mass spectrometry does not show any product formation at all, accompanied by no observed change in roughness. The H-terminated surface is apparently stable to the incoming XeF_2 molecules and etching does not start immediately. Next, the roughness layer thickness shows an initial rapid increase in roughness. Simultaneously, the production coefficient increases rapidly. After $\sim2\times10^3$ ML of XeF_2 dose the roughening slows down appreciably, accompanied by a slowly decreasing production coefficient. In the beginning, the top layer is thinner than the bottom layer but increases more rapidly. The top layer even becomes thicker than the bottom layer for a certain period of time. Beyond 3×10^3 ML of XeF_2 dose, the bottom layer is again thicker than the top layer.

This behavior can be explained qualitatively as follows. The H termination prevents etching to start immediately. This implies that H is not replaced by F. First, H has to be removed, presumably through SiH_xF_y product formation. The F atoms have to insert into Si–Si backbonds for etching to take place. The SiH_xF_y product formation is apparently difficult and delays the start of etching. The SiF_4 product

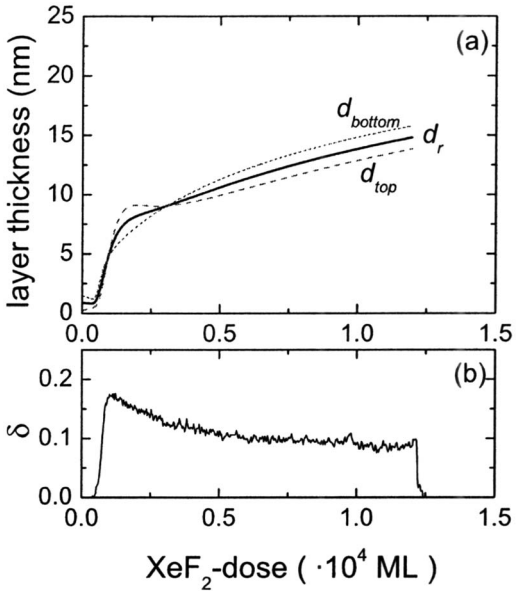

FIG. 4. (a) Roughness layer thickness d_r (solid line) as a function of XeF_2 dose of an initially H:Si(100) sample. Also shown are the top-layer thickness d_{top} (dashed line) and the bottom-layer thickness d_{bottom} (dotted line) from the two-layer roughness model, which add up to d_r, following the weighting formulism presented in Sec. IV. (b) Production coefficient δ as a function of XeF_2 dose, as measured by mass spectrometry simultaneously during the ellipsometry measurement.

formation at Si sites, which have been cleared from H, is no longer hampered and the etching can begin. This will lead to preferential etching in depth at H-free areas on the surface, i.e., SiF_x surface patches, hence the roughness grows rapidly. The size of the SiF_x patches grows less rapid than the roughness layer thickness, which leads to pitting of the surface. If the lateral dimensions of the pits grow slower than the depth, i.e., d_r, a significant increase in the number of surface sites where XeF_2 can react is to be expected. As a result SiF_4 product formation increases rapidly. Slowly the remaining H-terminated surface area is being removed and etch pits start merging. The pitlike surface eventually changes into a surface with cusplike roughness features. Characteristic for such a surface is a bottom-layer thickness larger than the top-layer thickness, as can be seen in the long term roughness evolution, i.e., the steady-state roughness growth, as shown in Fig. 4(a). The slowly decreasing δ after the initial rapid increase is not fully understood. A similar dose dependence of δ was observed by Vugts *et al.*[6] It is most likely related to a slight decrease in the surface area after the initial rapid increase in surface area associated with the influence of surface H atom and deep etch pits. The H termination has forced the surface morphology into a state which is not alike the natural, stochastic roughness evolution for XeF_2 etching of clean Si(100). Once the influence of surface H atoms has disappeared, the etch process may strive to restore the surface morphology natural for XeF_2 etching of Si(100). When etch pits broaden and grow together possibly also the reduced confinement of XeF_2 within the etch pits may play a role. Also, SiF_3^+ signal assumed to be caused by SiF_4 etch products may partially be originating from SiF_3H etch products, which require less F atoms to create volatile etch products. The latter is however not likely the reason for the overshoot and decrease in δ. From the integration of δ the Si etch yield can be determined.[3] The etch yield related to SiF_3H_y should then be equal to the area under the δ curve that exceeds the steady-state (=long XeF_2 exposure) level of 0.09 ± 0.02. The Si etch yield related to this area is $\sim$80 ML and is therefore much larger than, at most, 2 ML of Si etch yield related to SiF_3H products.

Figure 5 shows a comparison between the weighted roughness layer thickness and atomic-force-microscopy measurements. As can be seen, the SE roughness d_r shows a similar trend as the atomic-force-microscopy (AFM) root-mean-square roughness σ. For long XeF_2-exposure time the SE roughness is approximately a factor of 2 larger than the AFM roughness. However, for shorter exposure time, more than a factor of 2 difference can be observed. Here, AFM tip-size effects are believed to underestimate the roughness in contrast to the SE roughness.[3] This, in fact, gives support to the proposed roughening mechanism as described above. If the lateral dimensions of the etch pits are below a critical size the AFM tip may not be able to properly track the surface height fluctuations.

The influence of crystal orientation was verified in an experiment subjecting a H:Si(111) (n-type, 4–16 Ω cm) to XeF_2. No quantitative difference in roughening and in production coefficient was observed between H:Si(100) and H:Si(111), which indicates that the roughening does not depend on crystal orientation at room temperature.

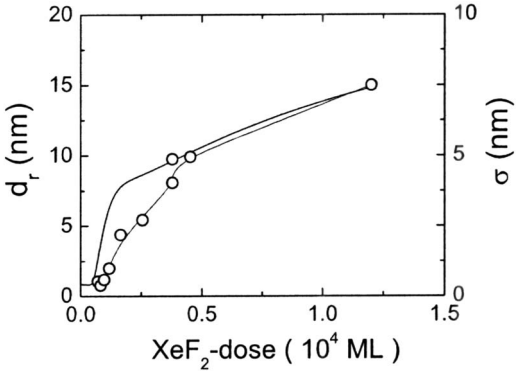

FIG. 5. Roughness layer thickness d_r (solid line) as function of XeF_2 dose compared to the root-mean-square roughness σ (open circles) obtained from AFM measurements on 10 H:Si(100) samples exposed to various XeF_2 doses. Note the factor of two difference in the scale for d_r (left) and σ (right).

VI. *A*-SI/SI(100) ETCHING

The etching of an a-Si layer on top of the c-Si bulk has been studied earlier by means of single-wavelength ellipsometry.[3] Here, we present a similar experiment, however with two differences: (a) spectroscopic ellipsometry is used to measure the etch process instead of single-wavelength ellipsometry, and (b) here a 6.4 nm a-Si layer is prepared by 1 keV Ar^+-ion bombardment instead of a 12 nm a-Si layer prepared by 2.5 keV Ar^+-ion bombardment. An impinging XeF_2 flux of 2.2 ML s^{-1} has been used. In Fig. 6(a) the a-Si/Si(100) roughening is shown together with the product formation [Fig. 6(b)] as a function of XeF_2 dose. The dotted, vertical line indicates where the layer modeling is

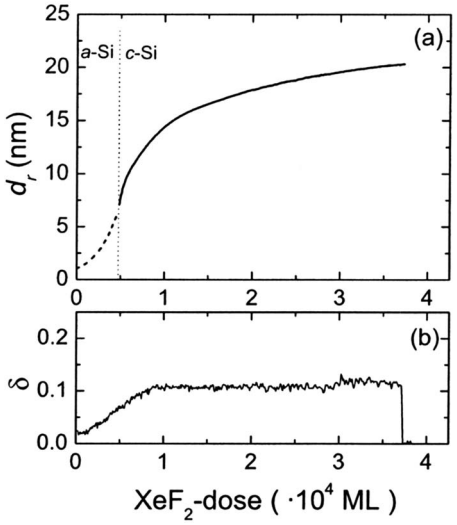

FIG. 6. (a) Roughness layer thickness d_r of a-Si (6.4 nm)/c-Si(100) as a function of XeF_2 dose. (b) Production coefficient δ as a function of XeF_2 dose, as measured by mass spectrometry simultaneously during the ellipsometry measurement.

switched from the *a*-Si, single-layer roughness model to the *c*-Si, two-layer roughness model. As can be seen, the weighted roughness layer thickness d_r is continuous, despite the fact that two totally different layer models are used to analyze the initial and long term SE measurements. Initially, the roughness shows a slow increase on the *a*-Si. Gradually the roughening speeds up and crosses over to a final, slower roughening phase. The production coefficient shows a low value of 0.03 when etching the *a*-Si, but increases to a final value of 0.11. The increase in the production coefficient coincides with the fast roughening phase and, thus, with the transition from *a*-Si to *c*-Si etching.

The reactive *a*-Si surface allows immediate bonding of F atoms. A reaction layer is created and hence the etching starts immediately. Etch product formation is observed and the roughness slowly increases. When going into the transition region, the absolute value of the roughness layer thickness becomes larger than in the H:Si(100) case. Here, the valleys of the rough *a*-Si reach the underlying *c*-Si bulk earlier than the hills. A preferential etching of *c*-Si over *a*-Si results in a large increase in d_r as etch pits are created in the *c*-Si. The roughness layer thickness grows in a rapid pace until all *a*-Si is removed. During this phase the production coefficient increases, partly because the number of surface sites where etching can occur increases on the walls of the etch pits and, partly because in the increase in the *c*-Si surface fraction with a larger δ than is the case for *a*-Si. Finally, δ levels off when only *c*-Si is being etched and the final, slower roughening phase is reached.

The spectroscopic ellipsometry result does not differ from the single-wavelength ellipsometry result in Ref. 3, except for the fact that the absolute roughness layer thickness after long XeF_2 exposure is higher in the single-wavelength ellipsometry measurements and the absolute value of the measured δ was somewhat lower due to calibration issues (see Sec. III). In the single-wavelength experiment a thicker amorphous silicon layer was initially created using 2.5 keV Ar^+ ions, resulting in an *a*-Si layer thickness of 12 nm. Thus, the moment at which the transition region will be reached, is shifted in time and more roughness will have accumulated on the *a*-Si. More *a*-Si roughness, i.e., the distance between hills and valleys, prior to entering the transition leads to thicker *a*-Si patches that have a longer lasting influence on the roughening in the etching of the *a*-Si/*c*-Si-interface. Hence, the absolute roughness layer thickness will be larger when a thicker *a*-Si layer is etched. The single-wavelength ellipsometry results reported in Ref. 3 are therefore in accordance with the SE results presented here and with the influence of the *a*-Si/*c*-Si-interface on the roughening behavior.

Top-view and cross-sectional SEM images have been taken of the sample in Ref. 3 that was exposed to 2×10^4 ML of XeF_2 (Fig. 7). The single-wavelength ellipsometric roughness layer thickness of this particular sample was measured to be 27.8 nm and an AFM root-mean-square roughness σ of 5.8 nm was found. The top-view SEM image [Fig. 7(a)] is indicative for the significant roughness of the sample surface and in the cross-sectional SEM image [Fig. 7(b)] evidence of high aspect ratio etch pits can be observed. Although these SEM images do not present conclusive evidence, they give support to the presented measurements and conclusions.

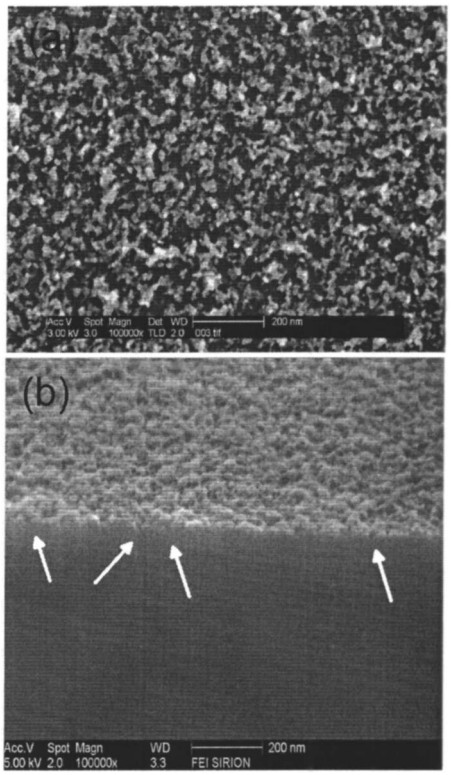

FIG. 7. (a) Top-view and (b) cross-sectional SEM images of the sample exposed to 2×10^4 ML of XeF_2. The images show significant roughness and in the cross-sectional view high aspect ratio etch pits can be observed.

VII. ROUGHENING, INITIAL CONDITIONS, AND REACTION LAYER

The cartoons in Fig. 8 summarize the roughening mechanism discussed for the two studies presented. On H:Si(100) the initial reaction is delayed (a), etch pits are created at surface positions where H is removed, resulting in a rapid increase in roughness layer thickness [(b)–(d)] and going into the final, slow roughening phase once all H is removed (e). On *a*-Si the roughness slowly increases (a), until valleys reach the underlying *c*-Si (b). A rapid increase in roughness layer thickness is caused by preferential etching of *c*-Si [(c) and (d)], until the *a*-Si patches are fully removed and the final, slow roughening phase is reached (e).

In both cases the interface layer plays a major role in the roughening behavior. The observed roughening indicates that Si(100) is preferentially etched over both H-terminated Si atoms and Si atoms in the amorphous material. As a result, when etching the interface layer, a fast roughening phase is observed. The absolute roughness prior to entering the final, slower roughening phase depends on how long the interface remains presents. The H:Si(100) interface is on the order of a monolayer thick and influences the etch process immediately at the start of XeF_2 exposure. The *a*-Si/Si(100) interface is on the order of a few to tens of monolayers depending on the

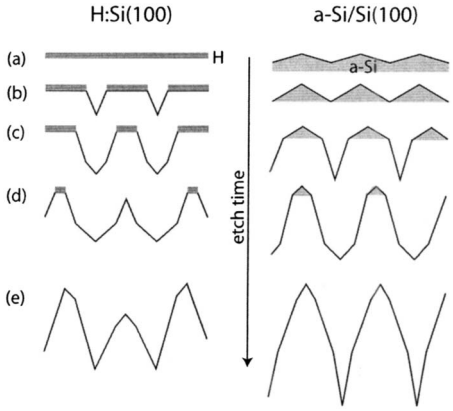

FIG. 8. Schematic representation of various phases of the roughening process on H:Si(100) (left) and *a*-Si/Si(100) (right) as described in previous sections. On H:Si(100) the initial reaction is delayed (a), etch pits are created at surface positions, where H is removed, [(b)–(d)] resulting in a rapid increase in roughness layer thickness (b)-(d) and going into the final, (e) slow roughening phase once all H is removed. (a) On the *a*-Si the roughness slowly increases, (b) until valleys reach the underlying *c*-Si. [(c) and (d)] A rapid increase in roughness layer thickness is caused by preferential etching of *c*-Si, until the *a*-Si patches are fully removed and (e) the final, slow roughening phase is reached.

roughness accumulated while etching the *a*-Si layer. Hence, the time duration of the influence of the interface, also the moment at which the fast roughening phase occurs, is determined by the thickness of the amorphous silicon after sputter cleaning. The observed absolute roughness before entering the final roughening phase is the lowest for the H:Si(100) interface and increases from the buried *a*-Si (6.4 nm)/Si(100) interface in this study to the *a*-Si (12 nm)/Si (100) interface in the single-wavelength study of Ref. 3.

The dose dependence of the production coefficient δ is shown to be most likely related to surface area changes for H:Si(100) etching, although the slow decrease after the initial rapid increase is not well understood. It is probably related to a restoration of the surface area increase, caused by the influence of surface H atoms, to a more natural surface morphology. For the *a*-Si/Si(100) etching the dose dependence of δ is partly related to surface area increase and partly by an etch rate difference between *a*-Si and *c*-Si. The observed δ after long XeF_2-exposure times is $\delta=0.09\pm0.02$ for H:Si(100) and 0.11 ± 0.02 for *a*-Si/Si(100), which supports the fact that the surface area increase after long exposure times is larger in the latter case. The exact surface area can be estimated if the (average) lateral dimension of the roughness features would be known. This information is however not available at present.

The observation of preferential etching of crystalline Si(100) over amorphous silicon is in contradiction with molecular dynamics (MD) simulations. MD suggest that *a*-Si etches more easily than *c*-Si.[19] If amorphous silicon is etched more easily than the crystalline silicon, it should lead to a delay, or even a decrease, in the roughening when etching through the amorphous-to-crystalline interface. The preferential etching of crystalline Si(100) over amorphous silicon, as concluded from the roughening behavior and production probability δ, is also observed under SF_6/O_2 plasma etch conditions by Zijlstra *et al.*[20] They attributed the etch rate difference to a higher oxygen content in the *a*-Si surface. In our case oxygen is not significantly present during the etching and can therefore not be held responsible for an etch rate difference here. To prove the preferential etching of crystalline Si(100) over amorphous silicon, the etching of a clean Si(100) sample should to be measured. Preparing clean Si(100) is however currently not possible in our setup.

In Sec. II we have discussed experimental observations of reaction layer thickness and composition. Furthermore, we have established that roughening of the surface occurs on time scales on the order of $0.5-10\times10^3$ ML of XeF_2 dose. In addition, different roughening behaviors as a function of XeF_2 dose has been observed and explained in relation to sample preparation, in particular, for HF dip and cleaning with ion bombardment. The SE and mass spectrometry study on H:Si(100) shows good agreement with the observations by Morikawa *et al.* First, the etch process is delayed by the H termination. Second, the observed roughening dynamics implies the creation of high aspect ratio etch pits and thus, an increase in the total number of surface atoms (=surface area increase). The fast roughening phase is observed on identical XeF_2-exposure times as the increase and change in composition of SiF_x species, as observed in x-ray photoemission spectroscopy (XPS) measurements.[2,7] We conclude that the surface morphology is an important aspect when measuring the reaction layer thickness and composition. Furthermore, the reaction layer thickness and composition may vary depending on the preparation method of the silicon substrates and the duration of XeF_2 exposure.

VIII. CONCLUSIONS

Spectroscopic ellipsometry has been applied to characterize surface roughening as a result of XeF_2 etching of interface layers on Si(100), in particular, H:Si(100) and *a*-Si/Si(100). The roughening shows in both cases initially a fast roughening followed by a slower roughening phase. The initial conditions of the surface prior to the etching, whether the surface is prepared by HF treatment or sputter cleaning by ion bombardment, have an important influence the roughening dynamics as a function of XeF_2-exposure time. The H-terminated Si(100) surface is stable to the XeF_2, which delays the onset of the etching. Consequently, surface regions where H atoms have been removed, are preferentially etched. This leads to a rapid increase in roughness layer thickness. Once all surface H atoms are removed, the roughening shows a slower, final roughening phase. A similar scenario is observed when etching the amorphous-to-crystalline silicon interface. Preferential etching of crystalline over amorphous silicon when etching through the *a*-Si/Si(100) interface results in a fast roughening phase. The roughness accumulated when etching the *a*-Si layer, which is proportional to the thickness of the initial *a*-Si layer, determines the duration of preferential etching and thus, the absolute roughness layer thickness at the end of the fast roughening phase.

These roughening mechanisms lead to high-aspect ratio etch pits and, as a result, a significant increase in the number of Si surface atoms, i.e., surface area increase. The corresponding surface morphology changes are of major influence on the SiF_4 product formation, i.e., etch rate, and the observed SiF_x reaction layer thickness and composition as measured with XPS.[2,7] Additionally, the presence of F ions in a surface region can play an important role during XeF_2 etching of Si (and consequently in the explanation of the reaction layer results in the literature), as recently addressed comprehensively by Winters *et al.*[10] Using very low energy ions to only remove the hydrogen bonding and subsequently evaluate the surface roughening during XeF_2 exposure in future experiments could conclusively provide full insight into the inhibiting effect of the H-termination.

ACKNOWLEDGMENTS

The authors wish to acknowledge J. A. C. M. van de Ven, L. H. A. M. van Moll, A. B. M. Husken, M. J. F. van de Sande, and J. F. C. Jansen for the technical support. This research was supported by The Netherlands Foundation for Fundamental Research on Matter (FOM:99TF24). The work of W.K. was made possible by the fellowship of the Royal Netherlands Academy of Arts and Sciences.

[1]D. Chen and J. J. Boland, Phys. Rev. B **70**, 205432 (2004).
[2]Y. Morikawa, K. Kubota, H. Ogawa, T. Ichiki, A. Tachibana, S. Fugimura, and Y. Horiike, J. Vac. Sci. Technol. A **16**, 345 (1998).
[3]A. A. E. Stevens and H. C. W. Beijerinck, J. Vac. Sci. Technol. A **23**, 126 (2005).
[4]P. G. M. Sebel, L. J. F. Hermans, and H. C. W. Beijerinck, J. Vac. Sci. Technol. A **17**, 755 (1999).
[5]J. W. Coburn and H. F. Winters, Surf. Sci. Rep. **14**, 161 (1992).
[6]M. J. M. Vugts, M. F. A. Eurlings, L. J. F. Hermans, and H. C. W. Beijerinck, J. Vac. Sci. Technol. A **14**, 2780 (1996).
[7]C. W. Lo, D. K. Shuh, V. Chakarian, T. D. Durbin, P. R. Varekamp, and J. A. Yarmoff, Phys. Rev. B **47**, 648 (1993).
[8]R. C. Hefty, J. R. Holt, M. R. Tate, D. B. Gosalvez, M. F. Bertino, and S. T. Ceyer, Phys. Rev. Lett. **92**, 188302 (2004).
[9]R. Q. Zhang, Y. L. Zhao, and Boon K. Teo, Phys. Rev. B **69**, 125319 (2004).
[10]H. F. Winters, D. B. Graves, D. Humbird, and S. Tougaard, J. Vac. Sci. Technol. A **25**, 96 (2007).
[11]1 ML of silicon fluoride is the equivalent of 1 ML of Si atoms with two F atoms per Si atom.
[12]David Humbird and David B. Graves, J. Appl. Phys. **96**, 791 (2004).
[13]Y. J. Chabal, G. S. Higashi, K. Raghavachari, and V. A. Burrows, J. Vac. Sci. Technol. A **7**, 2104 (1989).
[14]P. G. M. Sebel, L. J. F. Hermans, and H. C. W. Beijerinck, J. Vac. Sci. Technol. A **18**, 2090 (2000).
[15]G. E. Jellison, Jr. and F. A. Modine, J. Appl. Phys. **76**, 3758 (1994).
[16]D. A. G. Bruggeman, Ann. Phys. **24**, 636 (1935).
[17]R. M. A. Azzam and N. M. Bashara, *Ellipsometry and Polarized Light* (North-Holland, Amsterdam, 1992).
[18]A. A. E. Stevens, W. M. M. Kessels, M. C. M. van de Sanden, and H. C. W. Beijerinck, J. Vac. Sci. Technol. **24**, 1933 (2006).
[19]D. Humbird and D. B. Graves, J. Vac. Sci. Technol. A **23**, 31 (2005).
[20]T. Zijlstra, E. van der Drift, M. J. A. de Dood, E. Snoeks, and A. Polman, J. Vac. Sci. Technol. B **17**, 2734 (1999).
[21]F. R. McFeely, J. F. Morar, N. D. Shinn, G. Landgren, and F. J. Himpsel, Phys. Rev. B **30**, 764 (1984).
[22]J. A. Yarmoff and F. R. McFeely, Phys. Rev. B **38**, 2057 (1988).